The Abdus Salam
International Centre for Theoretical Physics

United Nations
Educational, Scientific and
Cultural Organization

IAEA
International Atomic Energy Agency

1859-3

Summer School on Novel Quantum Phases and Non-Equilibrium Phenomena in Cold Atomic Gases

27 August - 7 September, 2007

Experiments with dipolar gases

Thierry Lahaye
University of Stuttgart

Experiments with dipolar quantum gases

Thierry Lahaye
5. Physikalisches Institut, Universität Stuttgart, Germany

August 9, 2007

Abstract

These lecture notes cover the material presented at the ICTP Trieste, for the summer school "Novel Phases and Non-equilibrium Phenomena in Cold Atomic Gases", and give an introduction to experiments with a dipolar quantum gas, namely a BEC of Cr atoms. After a short discussion on the experimental realization of such a gas, emphasis is put on two interesting aspects of dipolar gases: dipolar relaxation, which prevents BEC of Cr in a magnetic trap but can be used for cooling a cloud of thermal atoms, and the anisotropic expansion of a dipolar BEC.

1 Introduction

Interactions play a crucial role in the physics of quantum gases (see, e.g., [1]). Usually they are isotropic and short-range, and proportional to the scattering length a of the atoms. The interatomic potential for this *contact interaction* can then be taken as :

$$U_{\text{contact}}(\boldsymbol{r}) = \frac{4\pi\hbar^2 a}{m}\delta(\boldsymbol{r}) \equiv g\delta(\boldsymbol{r}). \tag{1}$$

With the dipolar interaction, it is possible to study quantum gases interacting via a *long range* and *anisotropic* potential

$$U_{\text{dd}}(\boldsymbol{r}) = \frac{C_{\text{dd}}}{4\pi}\frac{1-3\cos^2\theta}{r^3}, \tag{2}$$

where C_{dd} is the dipolar coupling constant ($C_{\text{dd}} = \mu_0\mu^2$ for magnetic moments μ, $C_{\text{dd}} = d^2/\varepsilon_0$ for electric dipole moments d), and θ the angle between direction joining the two dipoles and the dipole orientation (we assume here that all dipoles are aligned along the same direction z).

Problem 1: Show by dimensional analysis that, for a gas with both contact and dipolar interactions, one can build a dimensionless parameter ε_{dd} quantifying the relative strength of both interactions, in which no length scale appears. We'll see later (problem 5) why it is convenient to choose the numerical factors in ε_{dd} in the following way:

$$\varepsilon_{\text{dd}} \equiv \frac{C_{\text{dd}}m}{12\pi\hbar^2 a}, \tag{3}$$

such that a homogeneous BEC with $\varepsilon_{\text{dd}} > 1$ is unstable.

2 Which dipolar gases?

One can think of two kinds of particles to realize experimentally a dipolar quantum gas: molecules having a permanent electric dipole moment d, or atoms having a large magnetic moment μ (I will not talk here about other, slightly different possibilities like using *induced* electric dipole moments in atoms).

2.1 Molecules

Heteronuclear molecules in their ground state can have large dipole moments, on the order of a few Debye ($1\,\text{D} \simeq 3.3\times10^{-30}\,\text{C}\cdot\text{m}$). For scattering lengths comparable to atomic ones, this yields ε_{dd} values in excess of 10^2. Such a dipolar quantum gas would therefore be completely dominated by dipolar effects; however, BECs of heteronuclear molecules in their ground state *are not available to date*[1].

[1] This might change soon with the many new experiments on mixtures of different species of fermions: using Feshbach resonances to create molecules and then transferring the molecules in their ground state could result in a dipolar molecular BEC. Let's mention also some molecule cooling techniques such as Stark deceleration or buffer-gas cooling, which have also the achievement of a dipolar BEC as one of their long-term goals.

2.2 Chromium

To date, the only quantum gas to display measurable dipolar effects is the Chromium BEC obtained in Stuttgart in 2004. Chromium has a large magnetic dipole moment of $6\mu_B$, and a scattering length of about $100a_0$ (a_0 is the Bohr radius). This gives $\varepsilon_{dd} \simeq 0.16$, which allows to observe a perturbative effect of the dipolar interaction.

Problem 2: Evaluate the value of ε_{dd} for ^{87}Rb atoms (the most common species for BEC experiments, having $\mu = \mu_B$ and a scattering length $a \simeq 5$ nm).

2.2.1 BEC of Chromium

In this section, I give a very brief overview of the experimental sequence used to obtain a ^{52}Cr BEC. More details can be found for example in [2].

The specific level structure of chromium makes it possible to use novel laser cooling strategies to load atoms continuously into a magnetic trap. After Doppler cooling in the magnetic trap, we get a cloud of 1.5×10^8 atoms at a temperature of a few hundreds of μK. RF-induced evaporative cooling is then performed. However, dipolar relaxation from the low-field-seeking state $|^7S_3, m_S = +3\rangle$ towards lower m_S states prevents condensation (see section 3.1).

The cloud (with 6×10^6 atoms at about 20 μK) is thus transferred into a crossed optical dipole trap (50 W at 1070 nm), and atoms are optically pumped to the high-field-seeking state $|^7S_3, m_S = -3\rangle$, which is the absolute ground state; with a magnetic field of a few Gauss, dipolar relaxation is thus energetically suppressed. Forced evaporative cooling in the dipole trap then yields a pure condensate with up to 10^5 atoms.

2.2.2 Feshbach resonances in Chromium

Besides its large magnetic moment, Cr has another asset: 14 Feshbach resonances have been observed [3] for atoms in the state $|^7S_3, m_S = -3\rangle$. Close to such a resonance, the scattering length varies with the applied magnetic field B as

$$a(B) = a_{bg}\left(1 - \frac{\Delta}{B - B_0}\right). \tag{4}$$

Here, B_0 is the resonance position, Δ its width, and a_{bg} the background (non-resonant) scattering length. This yields the possibility of increasing ε_{dd} by making a approach zero. For this, one needs to control the magnetic field B with a precision much better than Δ. The broadest known Feshbach resonance of Cr lies at $B_0 = 589$ G, and has a width of $\Delta = 1.4$ G. The small value of $\Delta/B_0 \simeq 2.3\times10^{-3}$ implies that one needs a good control of the field ($\lesssim 10^{-4}$) to tune a accurately.

3 Dipolar relaxation: enemy or ally?

3.1 Losses

One of the various types of two-body inelastic losses[2] arising in ultracold cloud of atoms is *dipolar relaxation*, i.e. a change in the spin projection of one or two of the colliding atoms, induced by the magnetic dipole-dipole interaction (2). Indeed, unlike e.g. spin-exchange collisions, which preserve the total spin, the anisotropic character of the MDDI allows for a change of the spin projection (only the *total* angular momentum, including the orbital part, needs to be conserved in the collision).

One can show that, within the Born approximation, the cross section for a single spin flip scales as S^3, where S is the spin of the atoms. Thus, although negligible for alkali atoms, dipolar relaxation is a very efficient loss mechanism for Chromium 52 ($S = 3$). Relaxation from the low-field seeking state (thus magnetically trapped) $|m_S = +3\rangle$ to the lower energy states $|m_S < +3\rangle$ prevents condensation of Cr in a magnetic trap (the dipolar relaxation coefficient is $\beta \sim 10^{-12}$ cm^3/s at low magnetic fields [4]). This can be circumvented by using an optical dipole trap (which traps all spin states) and optically pumping the atoms to the absolute ground state $|m_S = -3\rangle$; with a high enough magnetic field $\mu B \gg k_B T$, dipolar relaxation is energetically suppressed and BEC can be achieved.

[2] Three-body losses are also of course important at large densities.

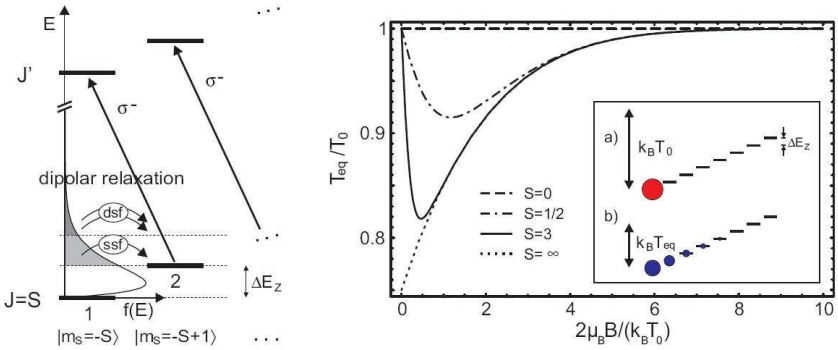

Figure 1: *Left: Principle of demagnetization cooling. Right: temperature reduction in a single demagnetization cooling step. Figure taken from [5].*

3.2 Demagnetization cooling

Theory. Dipolar relaxation introduces a coupling between spin and external degrees of freedom. It can thus be used to cool an atomic cloud by letting a sample, initially polarized in the lowest energy state (in a field $B_0 \gg k_B T_0/\mu$, where T_0 is the cloud temperature), relax towards full thermal equilibrium at a field $B_1 \sim k_B T_0/\mu$: energy is then absorbed by the spin reservoir at the expanse of the kinetic energy (see figure 1). The temperature of the sample thus decreases, by an amount which can be up to a few tens of percents. By optical pumping, the sample can be polarized again, and a new cycle can begin.

Problem 3: Toy model of single-step demagnetization cooling. Consider a thermal cloud of spin 1/2 atoms (with a Landé factor $g = 2$), in a harmonic trap.

(i) Show that at temperature T and magnetic field B, the internal energy per particle (due to spin degrees of freedom) is $U_{\rm spin} = -\mu_B B \tanh[\mu_B B/(k_B T)]$.

(ii) What is the energy per particle due to the center of mass motion in the harmonic trap (hint: use the equipartition theorem)?

(iii) One starts with a gas sample at temperature T_0, in a field $B_0 \gg k_B T_0/\mu_B$, polarized in the lowest energy spin state. One then reduces the field to the value B_1. Find the new temperature T_1 of the system after dipolar relaxation to equilibrium, as the solution of a transcendental equation. Plot T_1/T_0 as a function of $2\mu_B B_1/(k_B T_0)$, and show that you recover the result of figure 1 (dash-dotted line).

In practice, one can use a continuous cooling scheme, with the optical pumping light always on, and a ramp in magnetic field. The interested reader is referred to [5] for details. This cooling mechanism is obviously reminiscent of the well-known adiabatic demagnetization used in solid state physics to cool down paramagnetic salts[3].

Experimental realization. This scheme has been successfully applied to Cr, allowing for a division of the cloud temperature by a factor of two (from 20 to 11 μK), with almost no atom loss [6]. This cooling is therefore much more efficient than evaporative cooling, where the decrease in atom number is large. An important figure of merit for cooling schemes in view of obtaining quantum degeneracy is the gain χ in phase-space density ρ per atom loss:

$$\chi \equiv -\frac{\mathrm{d}\ln\rho}{\mathrm{d}\ln N}. \tag{5}$$

For evaporative cooling, χ is limited in practice[4] to values about 4. In [6], the measured efficiency of demagnetization cooling reached $\chi \simeq 11$.

The practical limitation in view of achieving lower temperatures lies essentially in the control of the polarization of the optical pumping light, as any residual σ^+ component yields a heating of the cloud. Note, however, that the recoil temperature should be attainable in principle with this technique.

[3] In a solid at low temperature, the specific heat of phonons is very small, making it possible to cool a sample by orders of magnitude in a single step.

[4] Using a higher evaporation threshold increases χ, but the evaporation time then increases prohibitively.

4 Dipolar expansion

The most spectacular effect of the magnetic dipole-dipole interactions (MDDI) on the Cr BEC in an anharmonic trap appears in time of flight experiments. The aspect ratio of the cloud during expansion is modified by the MDDI and depends on the orientation of the atomic dipoles with respect to the trap axes. In this section I first give a summary of the theoretical tools used to describe such experiments, and then describe our results.

4.1 GPE for dipolar gases

Pure contact interaction: a reminder. Let's recall that weakly interacting BECs with pure contact interaction are well described by the Gross-Pitaevskii equation (GPE) for the order parameter $\psi(\boldsymbol{r},t)$:

$$i\hbar\frac{\partial\psi}{\partial t} = -\frac{\hbar^2}{2m}\triangle\psi + \left(V_{\text{ext}} + g|\psi|^2\right)\psi. \tag{6}$$

The non-linear term proportional to g accounts for the effect of interactions within the mean-field approximation. Note also that in the time-independent case, the left-hand side of the above equation has to be replaced by $\mu\psi$, with μ the chemical potential. The normalization of ψ chosen here is $\int|\psi|^2 = N$, where N is the total atom number.

A useful reformulation of the Gross-Pitaevskii equation is obtained by writing $\psi = \sqrt{n}\exp(iS)$, with n the atomic density and S the phase of the order parameter, related to the superfluid velocity field by $\boldsymbol{v} = (\hbar/m)\boldsymbol{\nabla}S$. Substituting in (6) and separating real and imaginary parts one gets the following set of hydrodynamic equations:

$$\frac{\partial n}{\partial t} + \boldsymbol{\nabla}\cdot(n\boldsymbol{v}) = 0, \tag{7}$$

the equation of continuity, and an Euler-like equation:

$$m\frac{\partial\boldsymbol{v}}{\partial t} + \boldsymbol{\nabla}\left(\frac{mv^2}{2} + gn + V_{\text{ext}} - \frac{\hbar^2}{2m}\frac{\triangle\sqrt{n}}{\sqrt{n}}\right) = \boldsymbol{0}. \tag{8}$$

Problem 4: Bogoliubov spectrum. For the case of a uniform condensate ($V_{\text{ext}} = 0$), show, by linearizing the hydrodynamic equations around equilibrium, that the frequency ω and wavevector k of a harmonic perturbation are linked by the following dispersion relation:

$$\omega = k\sqrt{\frac{gn}{m} + \frac{\hbar^2k^2}{4m^2}}. \tag{9}$$

Dipolar interaction. To include dipolar effects, one just needs[5] to add an extra term to the mean-field potential $g|\psi|^2$, namely

$$\Phi_{\text{dd}}(\boldsymbol{r},t) = \int|\psi(\boldsymbol{r}',t)|^2\,U_{\text{dd}}(\boldsymbol{r}-\boldsymbol{r}')\,\mathrm{d}^3r'. \tag{10}$$

This extra term is thus *non-local* (due to the long-range character of the MDDI) and makes it much more complicated to solve the GPE, even numerically (one faces now an integro-differential equation).

Problem 5: Phonon instability for $\varepsilon_{\text{dd}} > 1$. Show the following identity:

$$\frac{1-3z^2/r^2}{r^3} = -\frac{\partial^2}{\partial z^2}\frac{1}{r} - \frac{4\pi}{3}\delta(\boldsymbol{r}). \tag{11}$$

Using this result, prove that the Fourier transform of the dipolar interaction (2) is

$$\widehat{U_{\text{dd}}}(\boldsymbol{k}) = C_{\text{dd}}(\cos^2\alpha - 1/3), \tag{12}$$

where α is the angle between $\boldsymbol{k}$ and the direction of the dipoles. Following the same method as in the previous problem, show that the excitation spectrum is now given by

$$\omega = k\sqrt{\frac{n}{m}\left[g + \frac{C_{\text{dd}}}{3}(3\cos^2\alpha - 1)\right] + \frac{\hbar^2k^2}{4m^2}}, \tag{13}$$

and that, with the definition (3) for ε_{dd}, this implies that a dipolar uniform condensate is unstable for $\varepsilon_{\text{dd}} > 1$.

[5] At least as long as the MDDI strength is not too high.

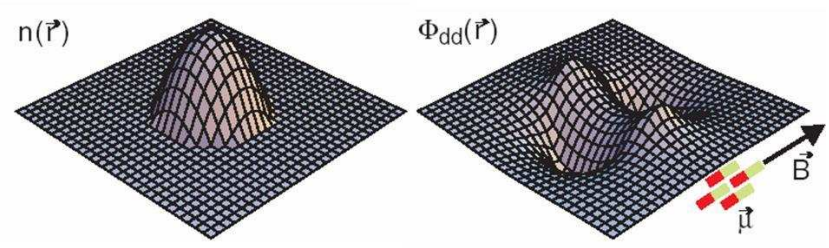

Figure 2: *Left: density distribution for a non-dipolar BEC in an isotropic trap. Right: the resulting dipolar potential* $\Phi_{\rm dd}$ *has a saddle-like shape, which tends to elongate the condensate along the magnetization direction. Figure taken from [8].*

4.2 Thomas-Fermi solutions and scaling Ansatz for the expansion

Static Thomas-Fermi solutions. For pure contact repulsive interaction, when the atom number is large, the condensate size increases and the zero-point kinetic energy becomes smaller and smaller. The Thomas-Fermi approximation consists in neglecting the kinetic energy term in the time-independent GPE; this gives then a simple algebraic equation, showing that the density distribution has the shape of an inverted parabola.

It is remarkable that this property remains valid if dipolar interaction is included. This comes from the fact that the dipolar mean-field potential $\Phi_{\rm dd}(\boldsymbol{r})$ for a parabolic density distribution $n(\boldsymbol{r}) = |\psi(\boldsymbol{r})|^2$ is quadratic in the coordinates (having a saddle shape because of the anisotropy). The proof of this property (which is not as trivial as it may seem) is left as the following problem.

Problem 6: Using the result (11), prove that

$$\Phi_{\rm dd}(\boldsymbol{r}) = -C_{\rm dd}\left(\frac{\partial^2}{\partial z^2}\phi(\boldsymbol{r}) + \frac{1}{3}n(\boldsymbol{r})\right), \quad \text{where} \quad \phi(\boldsymbol{r}) = \int \frac{n(\boldsymbol{r}')}{4\pi|\boldsymbol{r}-\boldsymbol{r}'|}\,\mathrm{d}^3r'. \tag{14}$$

The last equality shows that the "potential" ϕ fulfills $\triangle\phi = -n$. Deduce from this the most general form of ϕ when one has a parabolic density distribution $n(\boldsymbol{r}) = n_0(1 - x^2/R_x^2 - y^2/R_y^2 - z^2/R_z^2)$. Prove finally that $\Phi_{\rm dd}$ has a parabolic shape. Using Gauss theorem, work out the exact expression of $\Phi_{\rm dd}(\boldsymbol{r})$ for a spherically symmetric inverted parabola density distribution (figure 2).

For the case of a spherically symmetric trap (and thus also a spherically symmetric density distribution for pure contact interaction), one can easily show that, to first order in $\varepsilon_{\rm dd}$, the effect of the MDDI is to elongate the condensate along the direction of magnetization: it is energetically favorable to accommodate new particles close to the magnetization axis, where $\Phi_{\rm dd}(\boldsymbol{r})$ is minimum (see figure 2), thus causing an elongation of the condensate. It is possible to show that this behavior is valid for anisotropic traps and for higher values of $\varepsilon_{\rm dd}$. Note however that for a non-spherical density distribution, calculating the coefficients of the quadratic terms in $\Phi_{\rm dd}$ is possible but very complicated, and beyond the scope of these notes. See [7] for details.

Expansion: scaling Ansatz. For a pure contact interaction, and in the Thomas-Fermi approximation ($Na/a_{\rm ho} \gg 1$, with $a_{\rm ho} = \sqrt{\hbar/(m\bar{\omega})}$), there exists a very useful solution of the GPE[6]. It shows that the inverted parabola shape of the condensate is maintained upon expansion (after release from the trap), with a mere *rescaling* of its radii. The scaling parameters $b_i(t)$ ($i = x, y, z$) giving the radii $R_i(t) = R_i(0)b_i(t)$ are solutions of the ordinary differential equations

$$\ddot{b}_i = \frac{\omega_i^2(0)}{b_i \prod\limits_{j\in\{x,y,z\}} b_j} \qquad (i \in \{x, y, z\}). \tag{15}$$

Like for the static case, this can be extended to the case of dipolar interactions, since $\Phi_{\rm dd}$ keeps a parabolic shape. The corresponding equations now read

$$\ddot{b}_i = \frac{\omega_i^2(0)}{b_i \prod\limits_{j\in\{x,y,z\}} b_j} + f(\{b_j\}; \{\omega_j\}; \varepsilon_{\rm dd}) \qquad (i \in \{x, y, z\}), \tag{16}$$

[6] Y. Castin and R. Dum, Phys. Rev. Lett. **77**, 5315 (1996); Yu. Kagan, E. L. Surkov, and G. V. Shlyapnikov, Phys. Rev. A **54**, R1753 (1996).

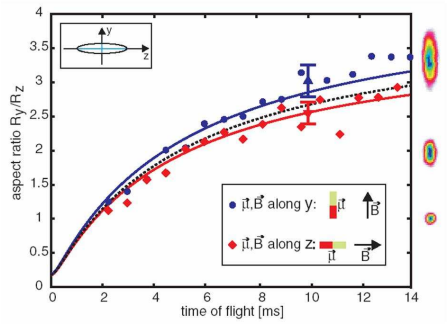

Figure 3: *MDDI as a small perturbation in the expansion of a condensate. The aspect ratio is measured during expansion for two different orientations of the dipoles with respect to the trap axes. Figure taken from [8].*

where f is a complicated function of the scaling radii, trap frequencies, and dipolar parameter $\varepsilon_{\rm dd}$. It turns out that the elongation of the condensate along the magnetization direction remains valid during expansion. The reader is again referred to [7] for further details.

4.3 Experiments

4.3.1 MDDI as a small perturbation

The first demonstration of an effect of the MDDI in a quantum gas came soon after the first realization of a Cr BEC, by measuring the aspect ratio of the BEC during time-of-flight for two different orientations of the dipoles with respect to the trap axes. The small value $\varepsilon_{\rm dd} \simeq 0.16$ implied that the effect was only a small perturbation on top of the expansion driven by the contact interaction (see figure 3).

4.3.2 Use of the Feshbach resonance

To go beyond this perturbative effect, we used the 589 G Feshbach resonance of Cr, in order to reduce a, and thus enhance $\varepsilon_{\rm dd}$. We provide this field using the offset coils of the magnetic trap, with a current of about 400 amperes, actively stabilized at a level of 4×10^{-5} in relative value (peak to peak). The field is switched on during the evaporation sequence in the ODT, at a stage when the density is not too high, in order not to lose too many atoms by inelastic losses when crossing the Feshbach resonances. The rest of the experiment is performed in high field. After a BEC is obtained, we ramp the field close to the resonance in 10 ms, hold the field there for 2 ms, and take an absorption picture (still in high field) after 5 ms of time of flight.

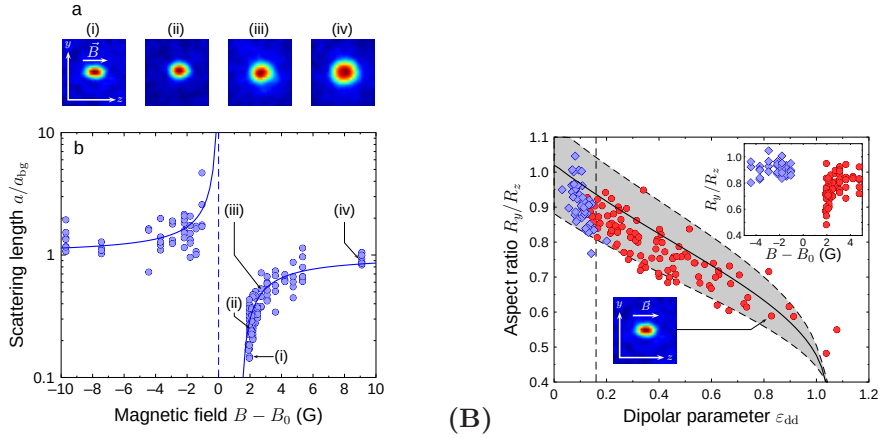

Figure 4: **(A)***: Measured scattering length $a(B)$ across the Feshbach resonance at $B_0 = 589$ G.* **(B)***: Aspect ratio of the BEC after 5 ms of expansion, as a function of the measured dipolar parameter $\varepsilon_{\rm dd}$. The solid line corresponds to the prediction of hydrodynamic equations in the Thomas-Fermi limit. Figure taken from [9].*

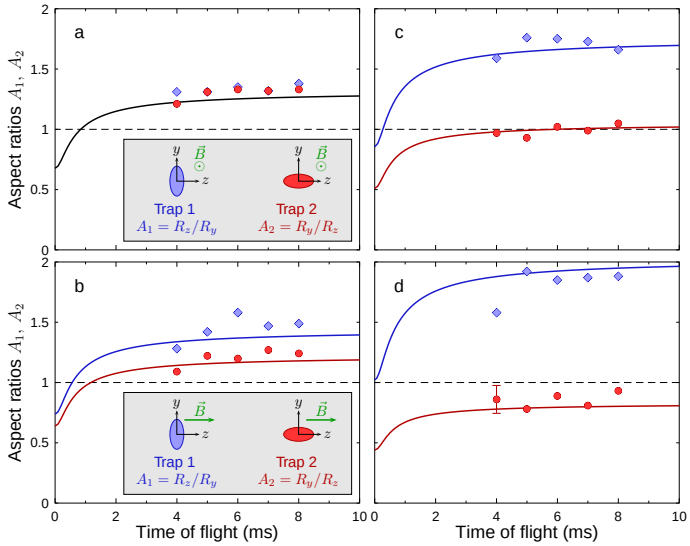

Figure 5: *Aspect ratio of the BEC vs time of flight. a:* $\varepsilon_{\rm dd} = 0.16$*, magnetic field along* x*, the aspect ratio is the same for the two trap configurations as expected. b:* $\varepsilon_{\rm dd} = 0.16$*, magnetic field along* z*, one basically recovers the results of figure 3. c:* $\varepsilon_{\rm dd} = 0.5$*. d:* $\varepsilon_{\rm dd} = 0.75$*, the inversion of ellipticity of the cloud is inhibited by the MDDI. Figure taken from [9].*

From the density distribution, we measure the Thomas-Fermi radii of the BEC, and we infer the value of the scattering length (taking into account explicitly the MDDI interaction by solving equations (16)). The measured a is shown on Fig. 4 (A). One can see clearly a five-fold reduction of a above resonance, corresponding to a maximal value of $\varepsilon_{\rm dd} \simeq 0.8$. On the sample absorption images of Fig. 4 (A), one clearly sees, when B approaches $B_0 + \Delta$, a strong reduction of the BEC size, due to the reduction of a, and thus of the mean field energy released upon expansion[7]. But one also clearly observes an elongation of the BEC along the magnetic field direction z. This change in the cloud aspect ratio would not happen for a pure contact interaction and is a direct signature of the MDDI. Fig. 4 (B) shows the aspect ratio of the cloud as a function of $\varepsilon_{\rm dd}$, together with the theoretical prediction from (16).

As an application of the tunability of $\varepsilon_{\rm dd}$, we measured the aspect ratio of the BEC during expansion for two different orientations of the dipoles with respect to the trap axes (as in the section 4.3.1). The effect of MDDI is now way beyond the perturbative regime (figure 5). For large enough $\varepsilon_{\rm dd}$, one clearly sees that the usual inversion of ellipticity of the BEC during expansion is inhibited by the MDDI.

5 Outlook

These lecture notes concentrated on properties of ultracold dipolar gases that have been already explored experimentally. On the theoretical side, many phenomena have been predicted, a short (and incomplete[8]) list of the studied subjects being:

- collective oscillations of dipolar BECs (frequency shifts due to MDDI predicted),
- equilibrium shape of the BEC in a harmonic trap (structured density profiles predicted),
- stability of the condensate (predicted to depend on the trap geometry, e.g. aspect ratio),
- rotating dipolar gases (with exotic vortex lattices predicted),
- low-dimensional dipolar gases (with e.g. new dispersion relations of excitations predicted),
- non-linear physics of dipolar gases (e.g. stable two-dimensional solitons predicted),
- dipolar fermi gases (new pairing mechanisms predicted),

[7] For a pure contact interaction, the TF radius after expansion scales as $(Na)^{1/5}$.
[8] See the lecture by Luis Santos for more details on the theoretical activities regarding dipolar quantum gases.

- dipolar quantum gases in optical lattices (new exotic quantum phases predicted, such as checkerboard or supersolid phases).

The field of ultracold dipolar gases thus remains barely explored experimentally, and many new exciting experiments are yet to come.

Acknowledgements

I thank the organizers of the summer school for giving me the opportunity to give these lectures in replacement of Tilman Pfau, and all my colleagues at the 5. Physikalisches Institut, Universität Stuttgart, for their contribution to my understanding of dipolar gases.

⋆ ⋆ ⋆

If you want to get the detailed solutions of the small problems given in these lecture notes, please send me an e-mail at:

t.lahaye@physik.uni-stuttgart.de.

References

[1] L. P. Pitaevskii and S. Stringari, *Bose-Einstein condensation*, (Clarendon Press, Oxford, 2003).

[2] A. Griesmaier, PhD thesis, Stuttgart University (2006).

[3] J. Werner *et al.*, Phys. Rev. Lett. **94**, 183201 (2005).

[4] S. Hensler *et al.*, Appl. Phys. B **77**, 765 (2003).

[5] S. Hensler *et al.*, Europhys. Lett. **71**, 918 (2005).

[6] M. Fattori *et al.*, Nature Physics **2**, 765 (2006).

[7] C. Eberlein *et al.*, Phys. Rev. A **71**, 033618 (2004); S. Giovanazzi *et al.*, Phys. Rev. A **74**, 013621 (2006).

[8] J. Stuhler *et al.*, Phys. Rev. Lett. **95**, 150406 (2005).

[9] T. Lahaye *et al.*, Nature (London) **449**, 672 (2007).

Experiments with dipolar quantum gases

T. Lahaye, T. Koch, B. Fröhlich, J. Metz,
M. Meister, A. Griesmaier, and T. Pfau

5. Physikalisches Institut, Universität Stuttgart

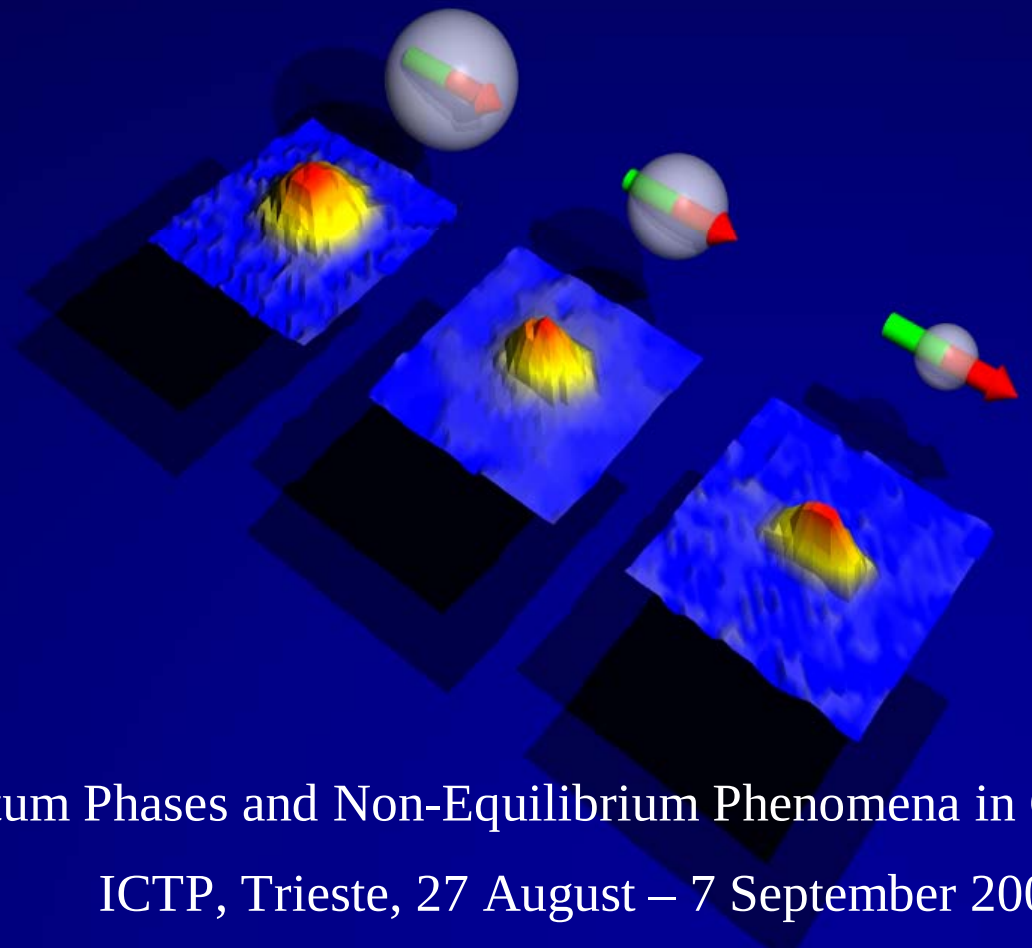

"Novel Quantum Phases and Non-Equilibrium Phenomena in Cold Atomic Gases"

ICTP, Trieste, 27 August – 7 September 2007

Interacting quantum systems in AMO physics

Contact interaction

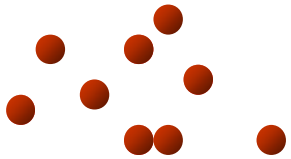

$$U_{\mathrm{vdW}}(\boldsymbol{r}) = \frac{4\pi\hbar^2 a}{m}\delta(\boldsymbol{r})$$

Short range
Isotropic

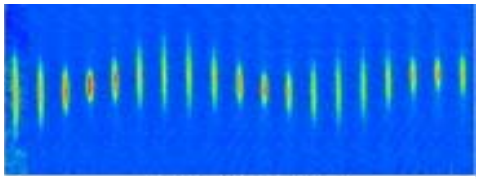

Dipole interaction

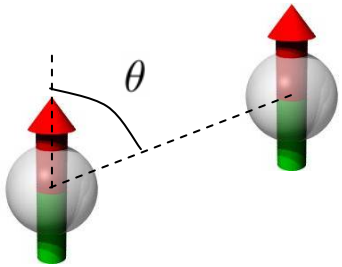

$$U_{\mathrm{dd}}(\boldsymbol{r}) = \frac{\mu_0}{4\pi}\mu^2\frac{1-3\cos^2\theta}{r^3}$$

Long range
Anisotropic

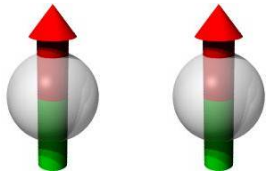

Repulsive

Coulomb interaction

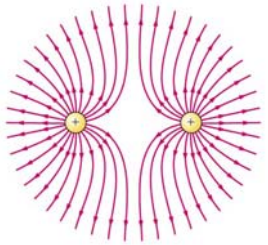

$$U_{\mathrm{Coul}}(\boldsymbol{r}) = \frac{q_1 q_2}{4\pi\varepsilon_0}\frac{1}{r}$$

Long range
Isotropic

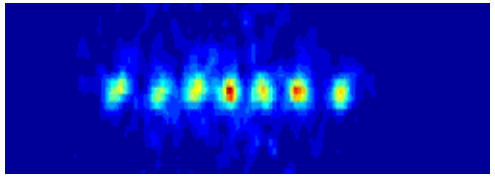

New physics in dipolar quantum gases

Dipole-dipole interactions are:

- anisotropic

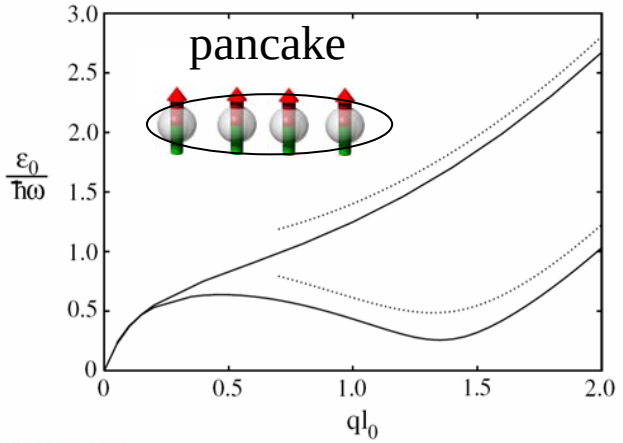

  - trap geometry-dependant stability
  - modified dispersion relation for elementary excitations (roton)
  - new equilibrium shapes

- long range

  - new quantum phases in optical lattices
    - supersolid
    - checkerboard

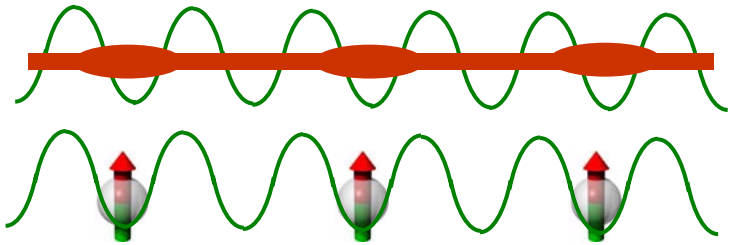

For an overview, see:

M. Baranov *et al.*, Physica Scripta **T102**, 74 (2002) + talk by Luis Santos this morning.

Outline

1. Which dipolar systems?

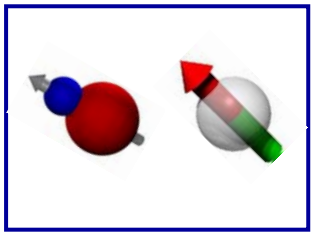

2. Demagnetization cooling

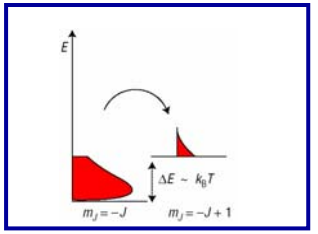

3. Expansion of a quantum ferrofluid

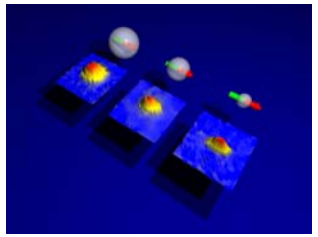

4. Dipolar collapse

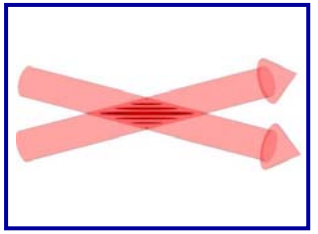

Outline

1. **Which dipolar systems?**

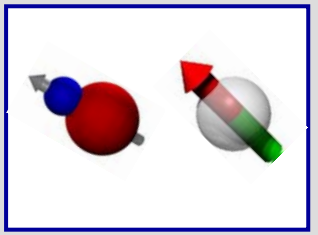

2. Demagnetization cooling

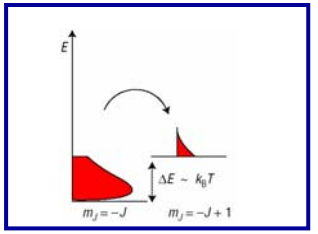

3. Expansion of a quantum ferrofluid

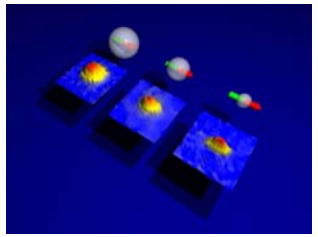

4. Dipolar collapse

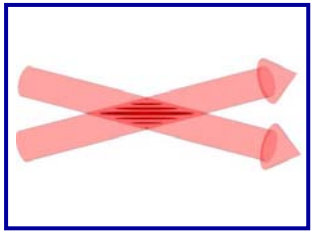

Dipolar systems in practice

Strength of the magnetic dipole-dipole interaction (MDDI):

$$\varepsilon_{\mathrm{dd}} = \frac{\mu_0 \mu^2 m}{12\pi\hbar^2 a}$$

Heteronuclear molecules (electric dipole moment d)

$$\mu_0\mu^2 \longrightarrow \frac{d^2}{\varepsilon_0}$$

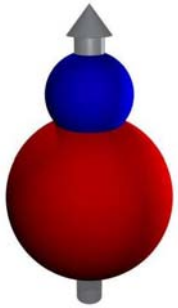

Large d (~1 Debye): $\varepsilon_{\mathrm{dd}} \sim 100$

No BEC yet

Atoms with large magnetic dipole moment μ.

Chromium: $6\mu_B$.

BEC achieved

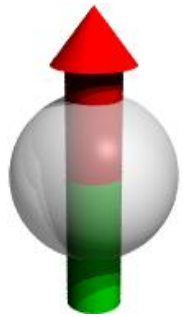

$$\varepsilon_{\mathrm{dd}} \simeq 0.16$$

Small $\varepsilon_{\mathrm{dd}}$… but a tunable

Chromium level scheme

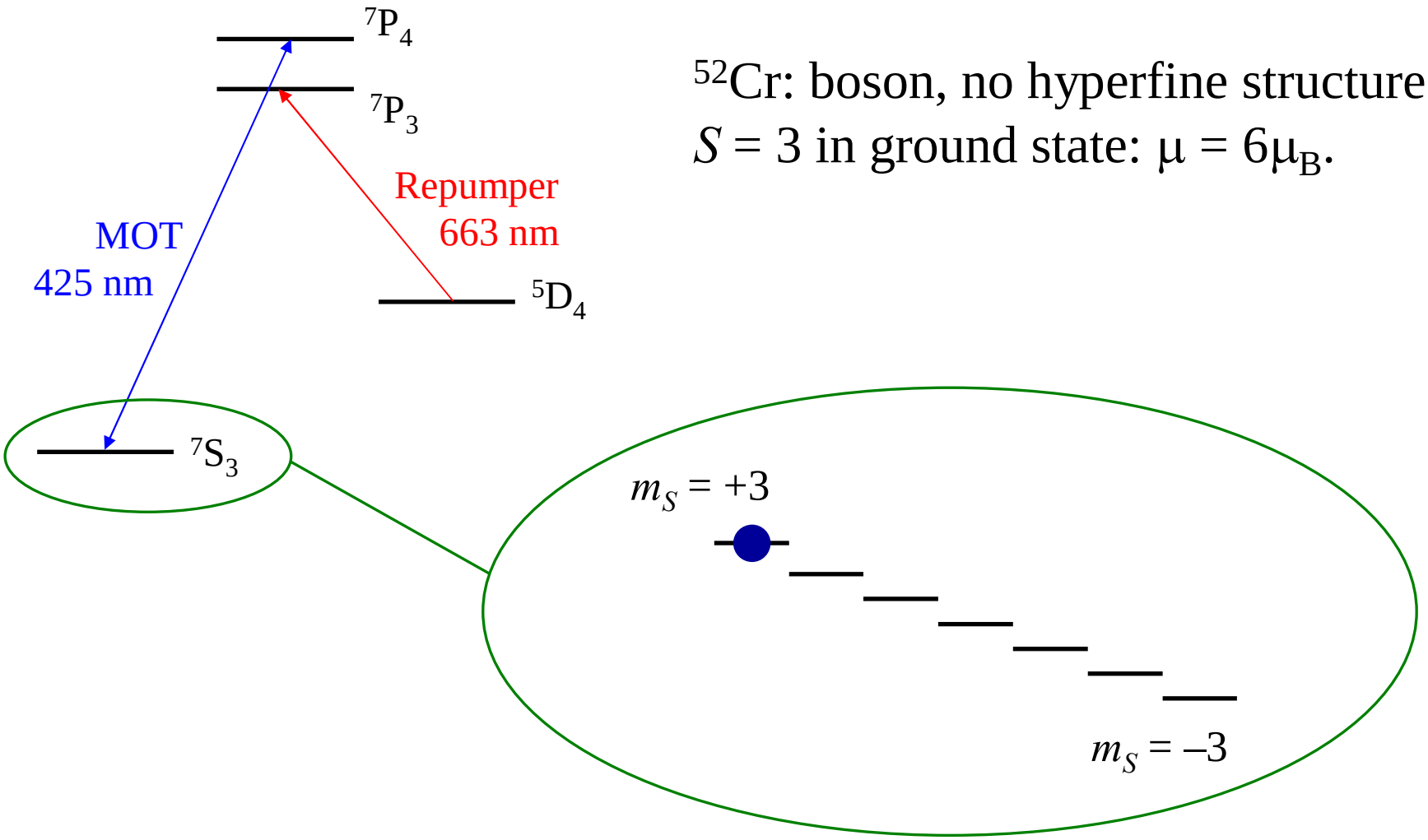

^{52}Cr: boson, no hyperfine structure

S = 3 in ground state: $\mu = 6\mu_B$.

Chromium BEC

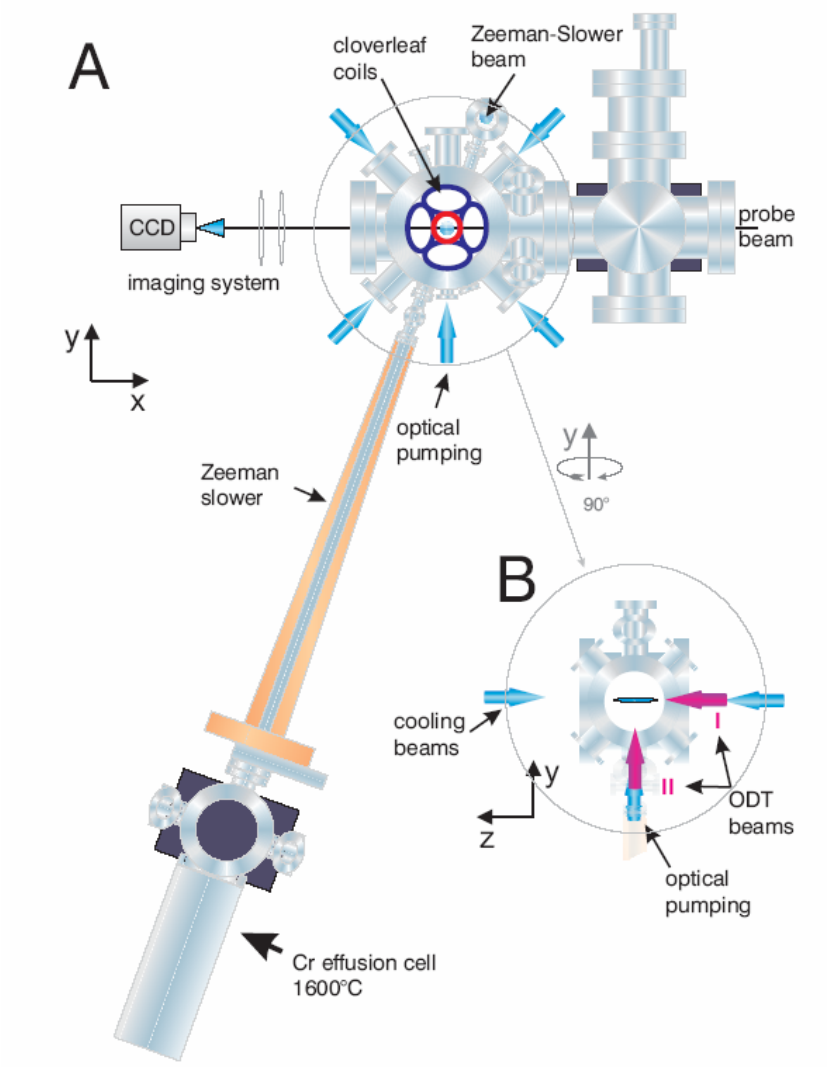

i. Continuous loading of a Ioffe-Pritchard trap.

ii. RF evaporation.

iii. Transfer to crossed ODT (50 W @ 1070 nm), optical pumping, and forced evaporation.

iv. 10^5 atoms in BEC!

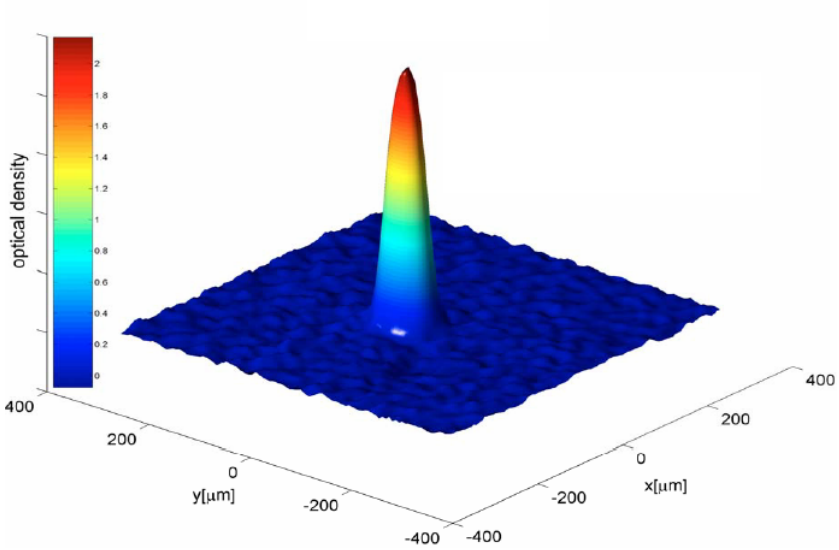

A. Griesmaier *et al.*, PRL **94**, 160401 (2005).

Feshbach resonances in Cr

Tuning of the scattering length with an external magnetic field:

$$a = a_{\mathrm{bg}}\left(1 - \frac{\Delta}{B - B_0}\right)$$

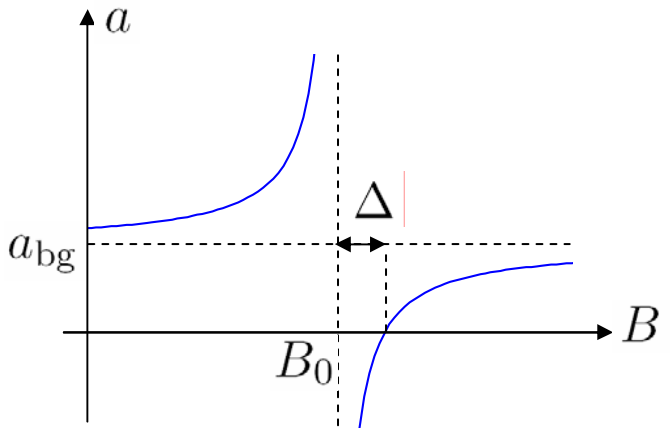

Feshbach resonances in Chromium [J. Werner *et al.*, PRL **94**, 183201, (2005)]

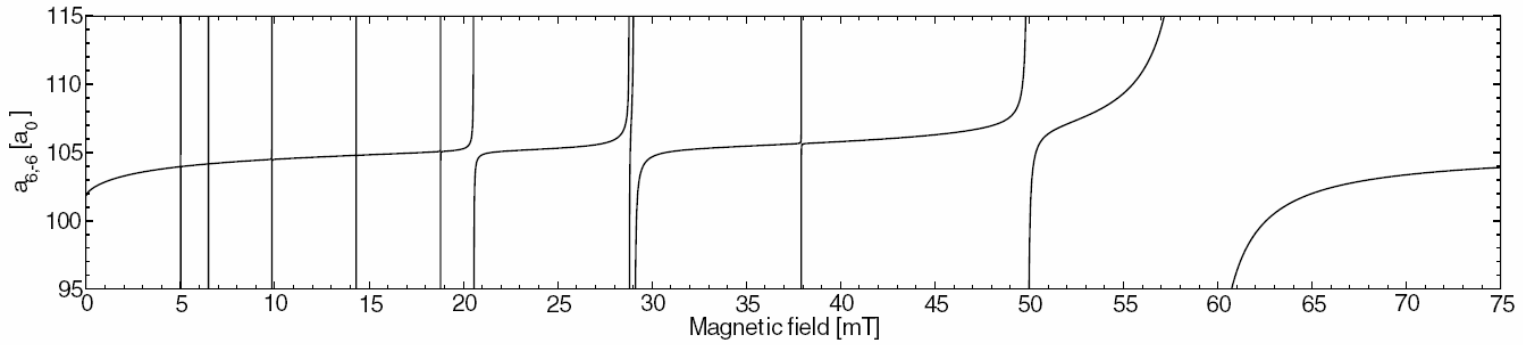

Broadest resonance at 589.1 G (Δ = 1.4 G):

Field stability better than 10^{-4} required!

Outline

1. Which dipolar systems?

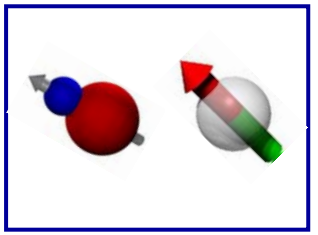

2. **Demagnetization cooling**

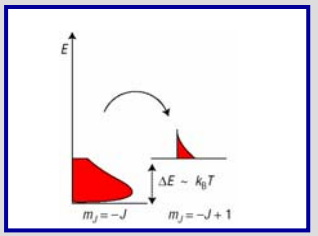

3. Expansion of a quantum ferrofluid

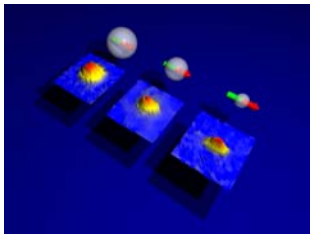

4. Dipolar collapse

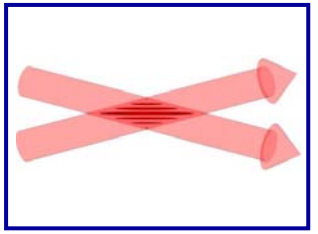

Dipolar relaxation

The dipolar interaction U_{dd} can induce spin flips:

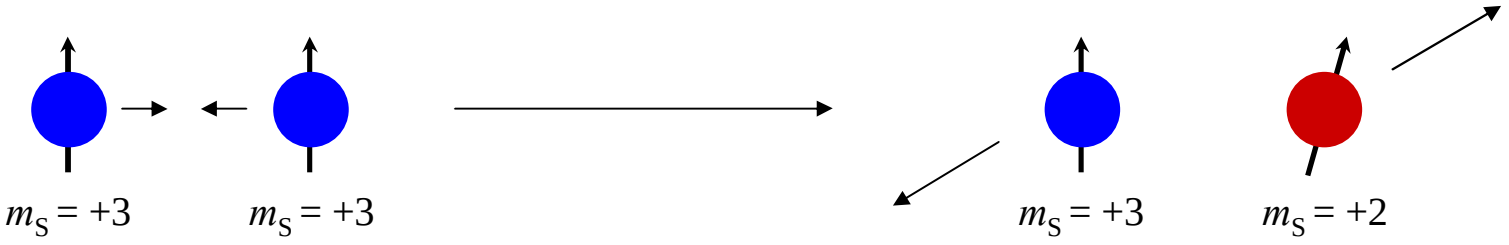

Cross-section proportional to S^3: huge loss mechanism for magnetically trapped ^{52}Cr ($S = 3$).

Loss rate : $\beta = 10^{-12}$ cm^3/s.

S. Hensler *et al.*, Appl. Phys. B **77**, 765 (2003).

Prevents BEC in $m_S = +3$.

Solution: optical trap, pump atoms in $m_S = -3$ and keep a field $\mu_B B >> k_B T$.

Demagnetization cooling: principle

(i) Start with all atoms in $m_J = -J$, at large field $\mu_B B_0 >> k_B T_0$.

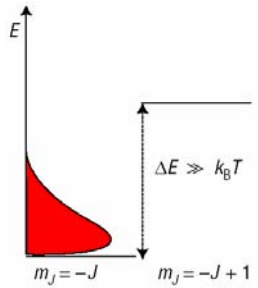

(ii) Reduce the field to $\mu_B B \sim k_B T_0$. Dipolar relaxation reduces E_{kin}.

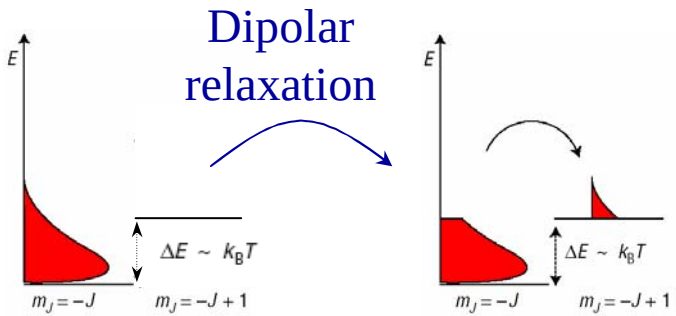

(iii) Apply optical pumping pulse to polarize again the cloud.

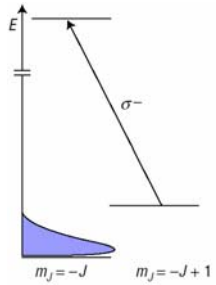

During step (ii), energy is conserved:

$$-g_J m_J \mu_B B + 3\, k_B T_0 = 3\, k_B T_{eq} + U_{spin}(B / T_{eq})$$

$$\rightarrow T_{eq} < T_0 : \text{Cooling!}$$

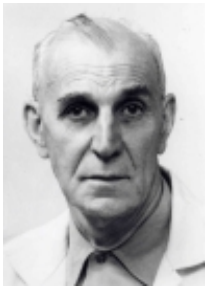

Scheme already discussed by Alfred Kastler ("effet lumino-frigorique").
A. Kastler, J. Phys. Radium **11**, 255 (1950).

Demagnetization cooling: principle

Temperature reduction for a single step:

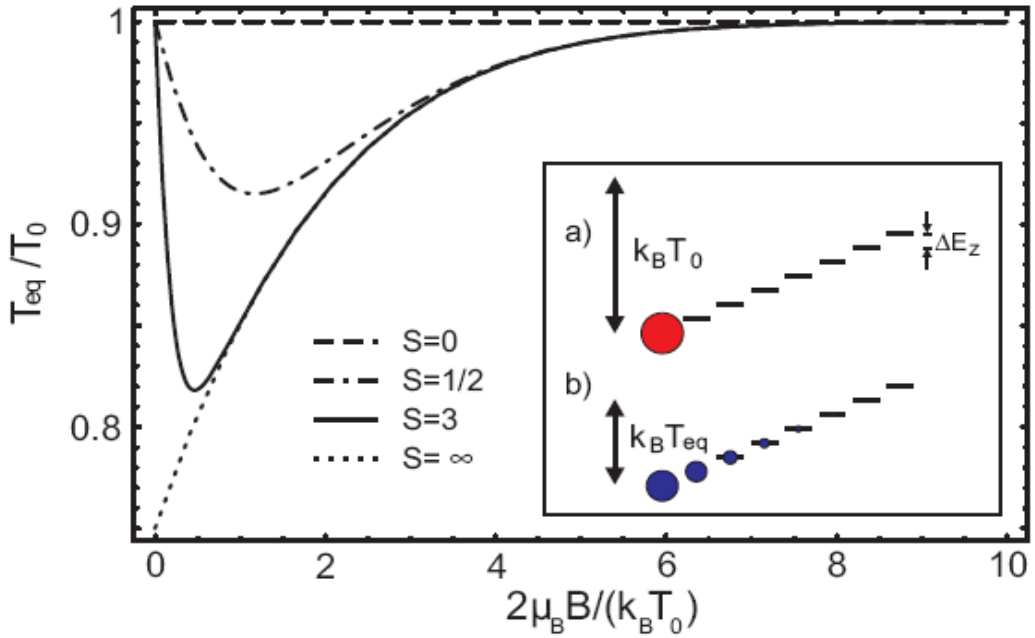

A continuous scheme with a ramp in *B* and the optical pumping light always on is possible.

Lower limit on *T*: ~ recoil limit (1 μK for ^{52}Cr).

S. Hensler *et al.*, Europhys. Lett. **71**, 918 (2005).

Demagnetization cooling: experiment

Single step:

B jumps from 1 G to 50 mG

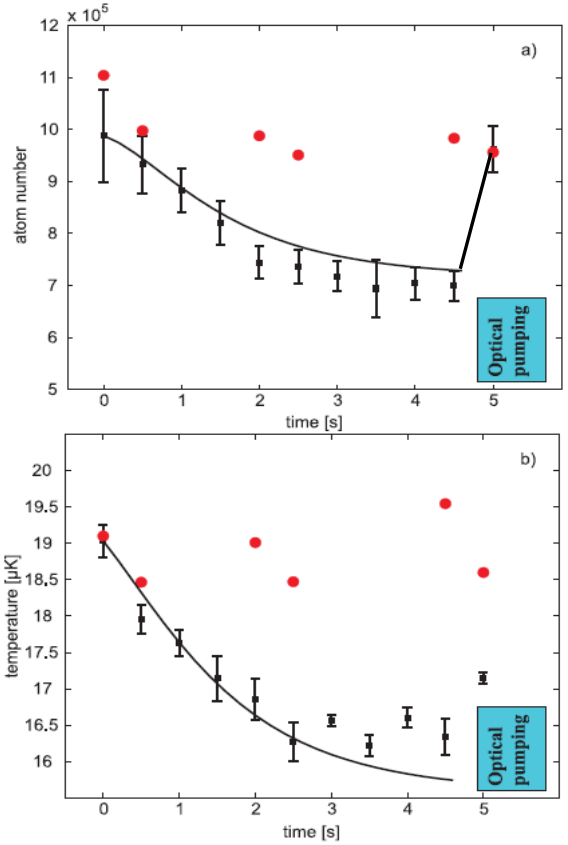

Continuous cooling:

B ramped down linearly from 250 mG to 50 mG over 7 s

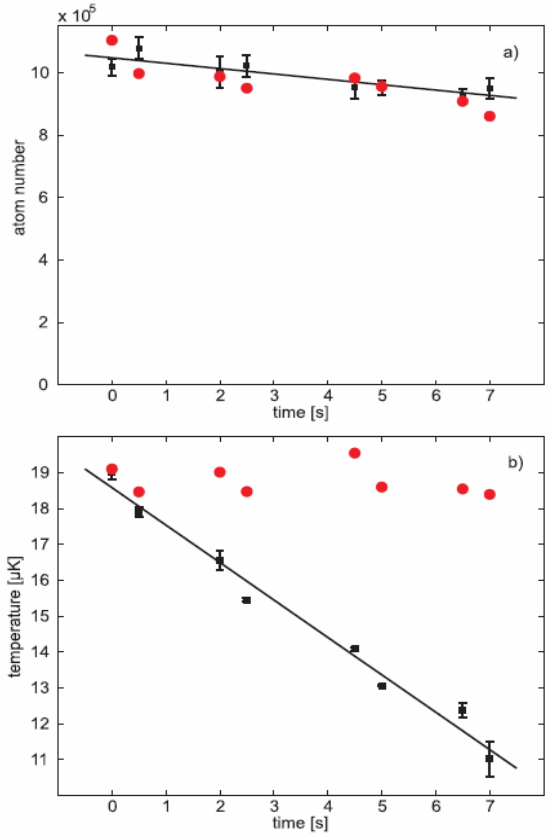

Cooling efficiency

$$\chi \equiv -\frac{\mathrm{d}\ln\rho}{\mathrm{d}\ln N}$$

$\chi = 11$

($\chi \sim 4$ in practice for evaporative cooling)

Temperature limit

10 μK experimentally: (difficult to control the σ^- polarisation of the optical pumping for very low $B \sim 50$ mG).

M. Fattori *et al.*, Nature Physics **2**, 765 (2006).

Outline

1. Which dipolar systems?

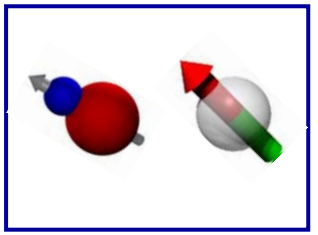

2. Demagnetization cooling

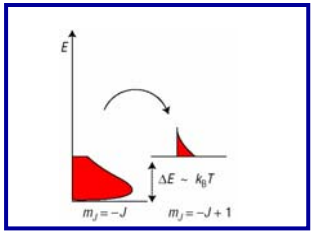

3. Expansion of a quantum ferrofluid

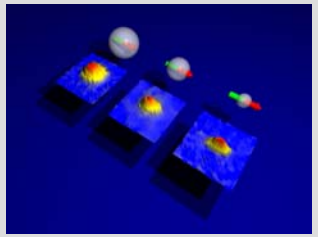

4. Dipolar collapse

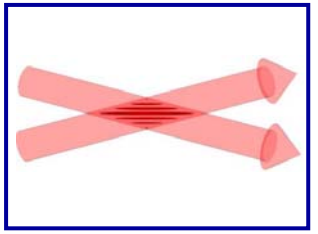

Gross-Pitaevskii equation with MDDI

Equation for the order parameter:

$$i\hbar\frac{\partial}{\partial t}\Psi(\vec{r},t) = -\frac{\hbar^2}{2m}\nabla^2\Psi(\vec{r},t) + V_{\rm ext}(\vec{r},t)\Psi(\vec{r},t) + \underbrace{V_{\rm mf}(\vec{r},t)}\,\Psi(\vec{r},t)$$

Interactions: non-linear term

$$n(\vec{r},t) = |\Psi(\vec{r},t)|^2$$

$$V_{\rm mf}(\vec{r},t) = g\,n(\vec{r},t) + \int d^3r' U_{\rm dd}(\vec{r}-\vec{r}')n(\vec{r}',t)$$

Contact interaction

Dipolar interaction

$$g = \frac{4\pi\hbar^2\,a}{m}$$

$$U_{\rm dd}(\vec{r}) = \frac{\mu_0\mu_{\rm m}^2}{4\pi r^3}\left(1 - \frac{3(\hat{e}_\mu\vec{r})^2}{r^2}\right)$$

Elongation of the BEC along the field

The MDDI elongates the BEC along the magnetization direction

Assume a spherical trap, and that ε_{dd} is small. To zeroth order, the density is then the usual inverted parabola:

$$n(\boldsymbol{r}) = n_0 \left(1 - \frac{r^2}{R_{\mathrm{TF}}^2}\right) \quad \text{for} \quad r \leqslant R_{\mathrm{TF}}$$

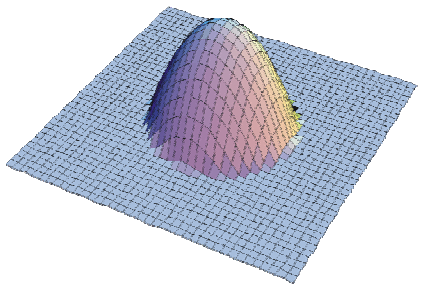

Mean-field potential due to dipole-dipole interactions:

$$\Phi_{dd}(\vec{r}) = \frac{\varepsilon_{dd} m \omega_0^2}{5}\left[1 - 3\left(\frac{\vec{e}_\mu \cdot \vec{r}}{|r|}\right)^2\right] r^2 \quad \text{for } r \leqslant R_{TF}.$$

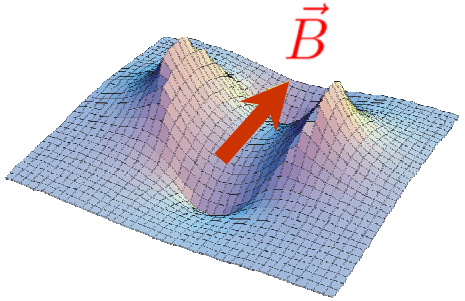

Saddle-shape potential

→ It is energetically favorable to accommodate atoms **close to the z-axis**.

This conclusion remains valid:

- ✓ for anisotropic traps,
- ✓ for arbitrary ε_{dd},
- ✓ during time-of-flight.

BEC expansion with a small dipolar perturbation

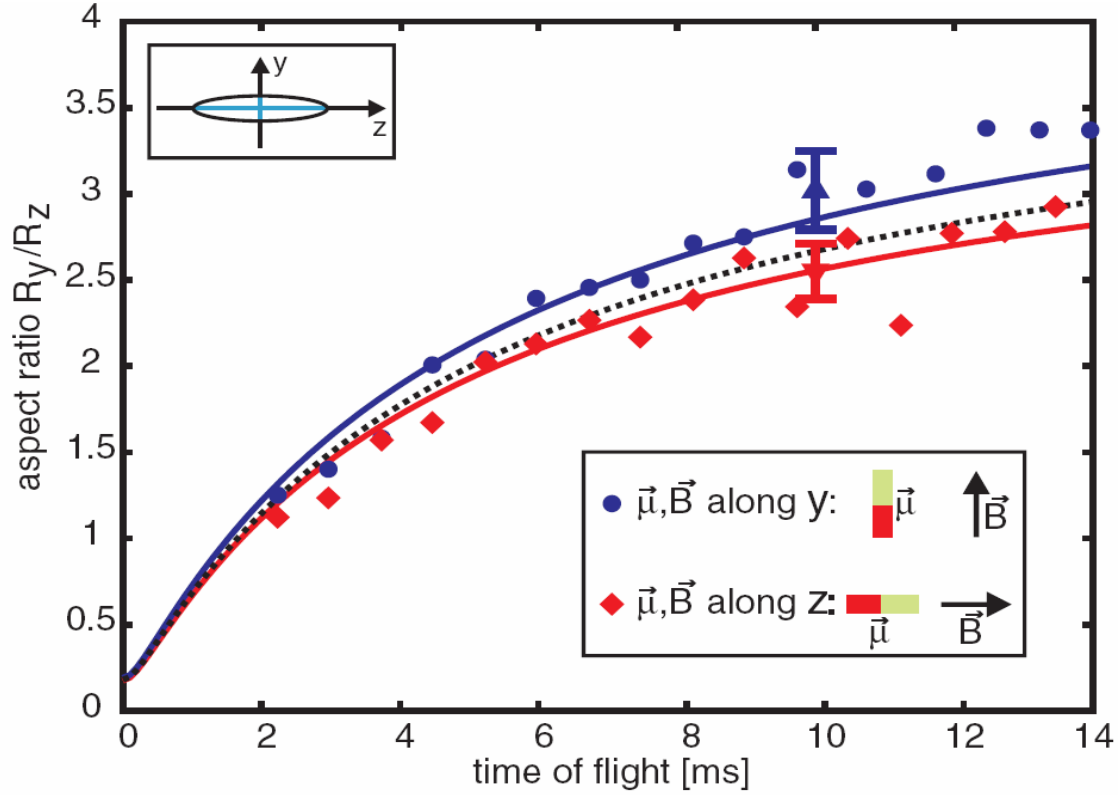

J. Stuhler *et al.*, Phys. Rev. Lett. **95**, 150406 (2005).

How to go beyond this perturbative effect? **Feshbach resonance!**

Modified experimental setup

Uniform field ~ 600 G

- ✓ offset 400 A + pinch 15 A (for curvature compensation)
- ✓ current actively stabilized at the 4×10^{-5} level (peak to peak)
- ✓ fast switching (2 ms)

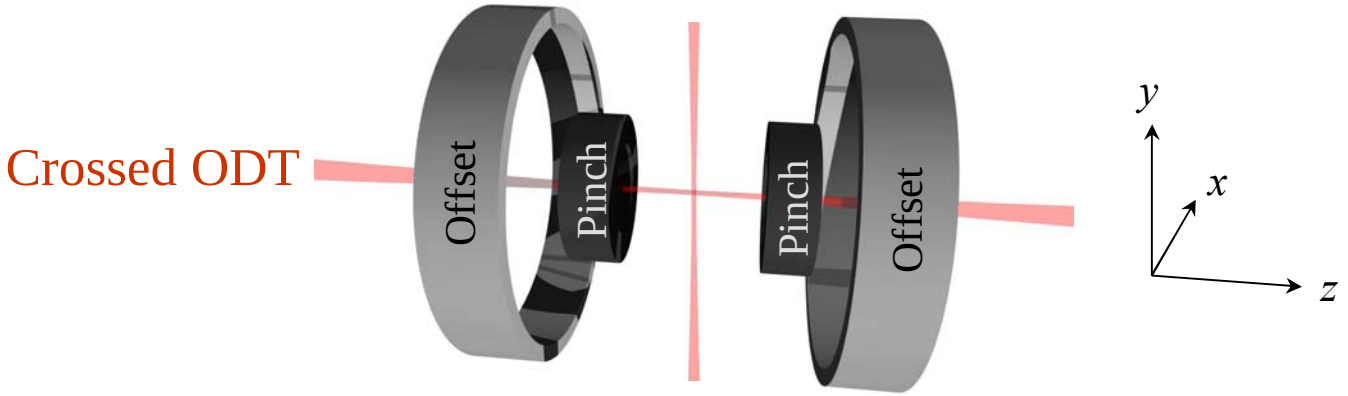

Absorption imaging in high field

- ✓ avoids to switch off *B* during time of flight

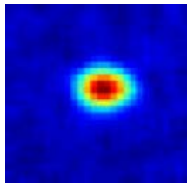

Experimental sequence

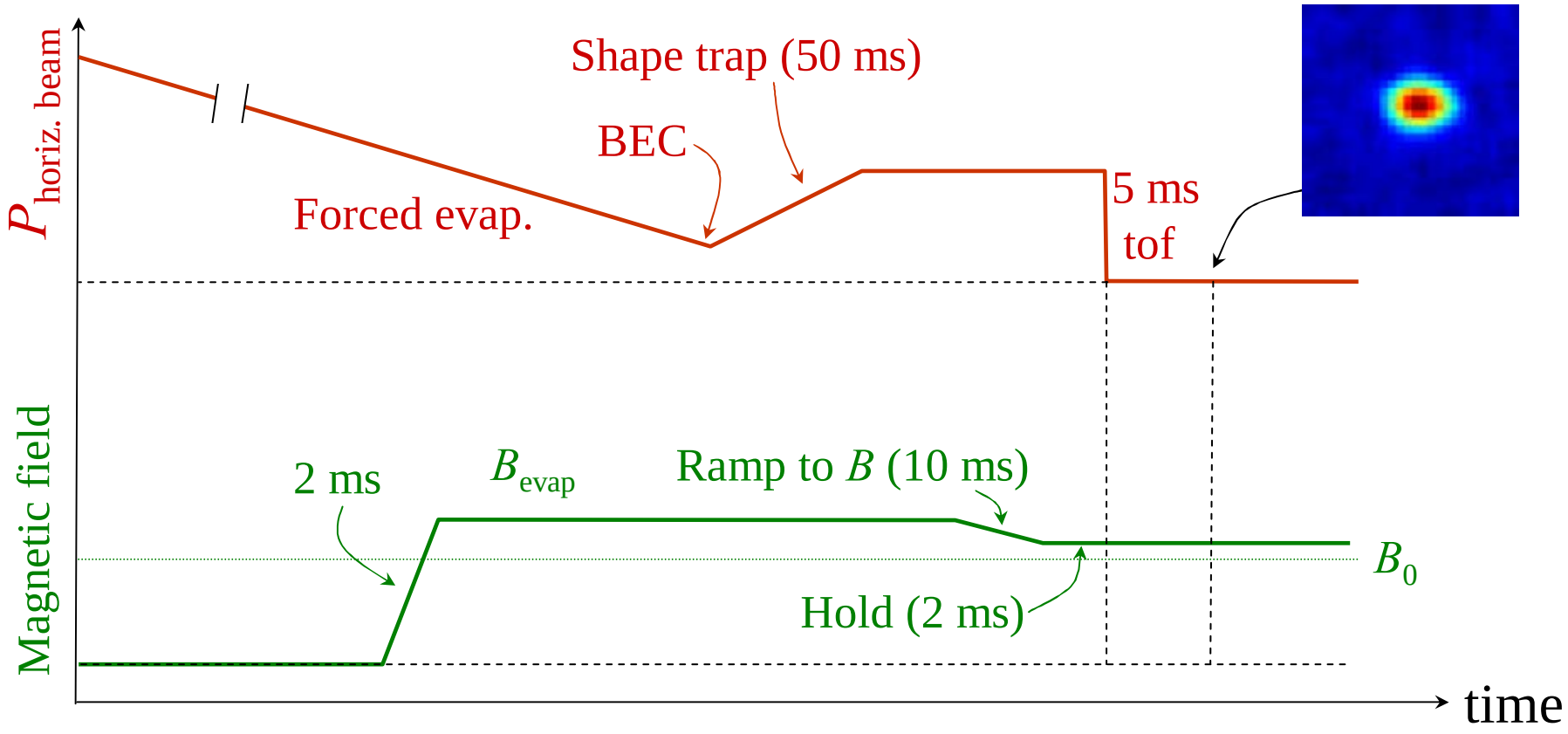

Tuning the scattering length

Without MDDI:
measure a through
the released energy

$$a \sim R^5 / N$$

Correction to take into account the MDDI.

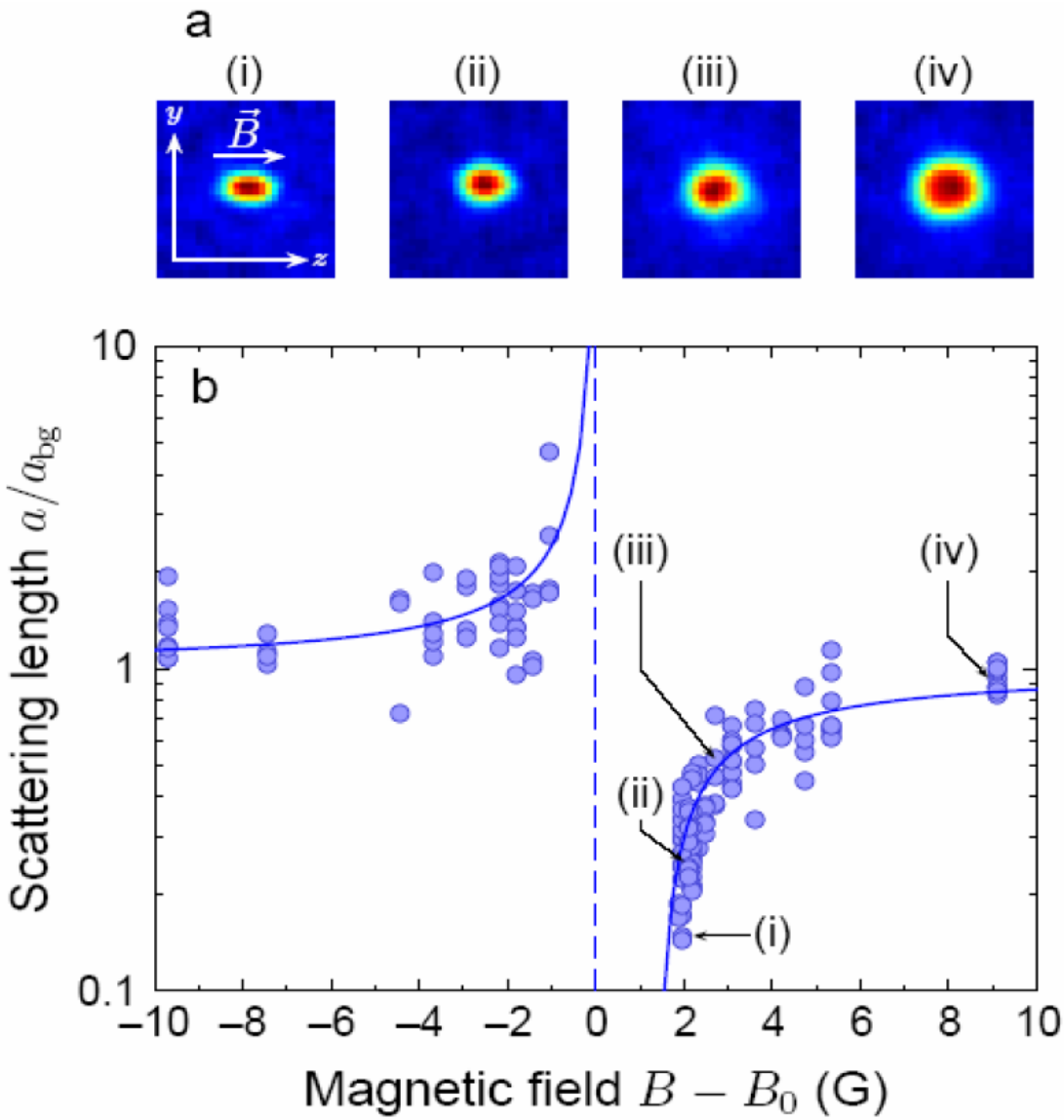

Aspect ratio vs. ε_{dd}

Dipole-dipole interactions: elongation along $\vec{B}$.

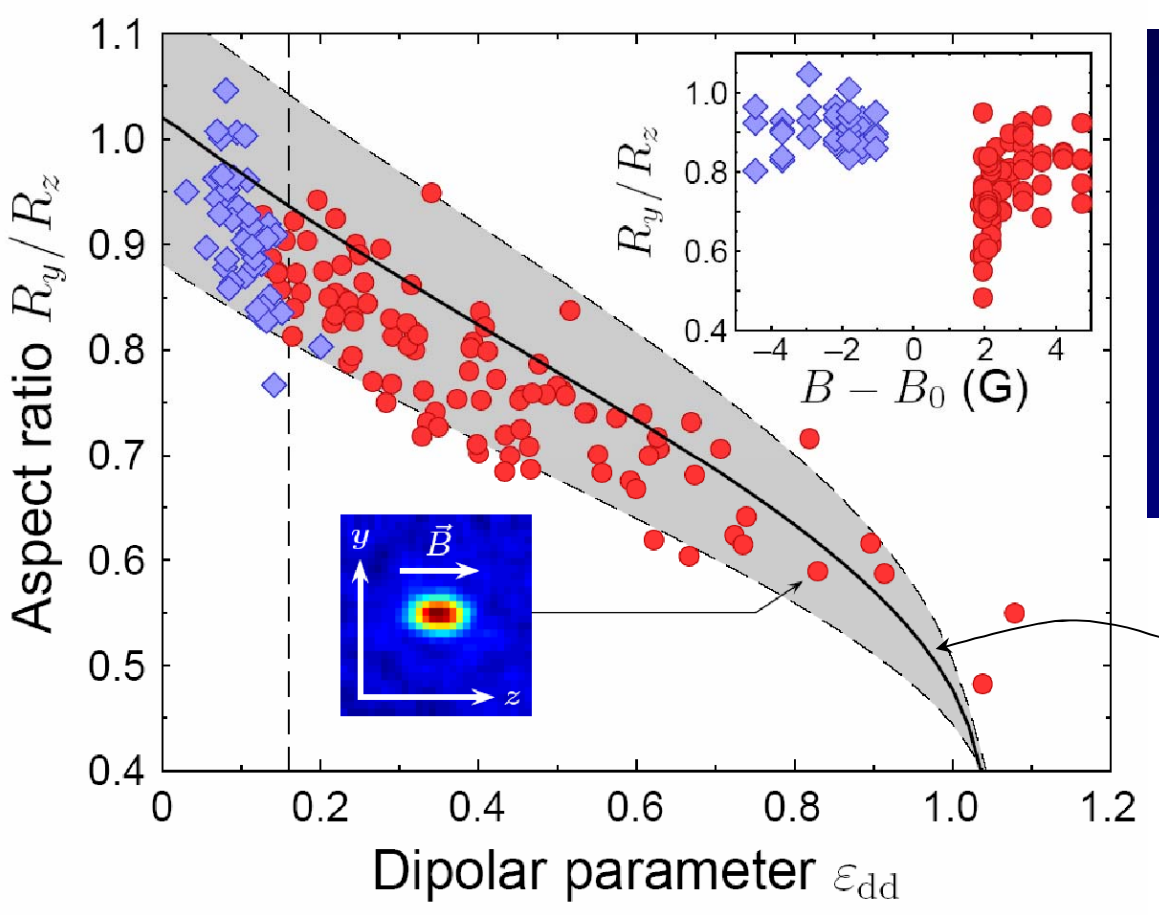

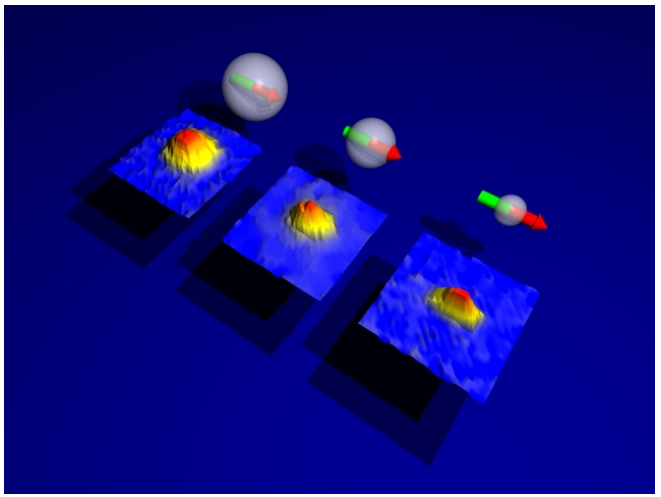

Hydrodynamics prediction
(no adjustable parameter)

T. Lahaye *et al.*, Nature **448**, 672 (2007).

Time of flight experiments for various ε_{dd}

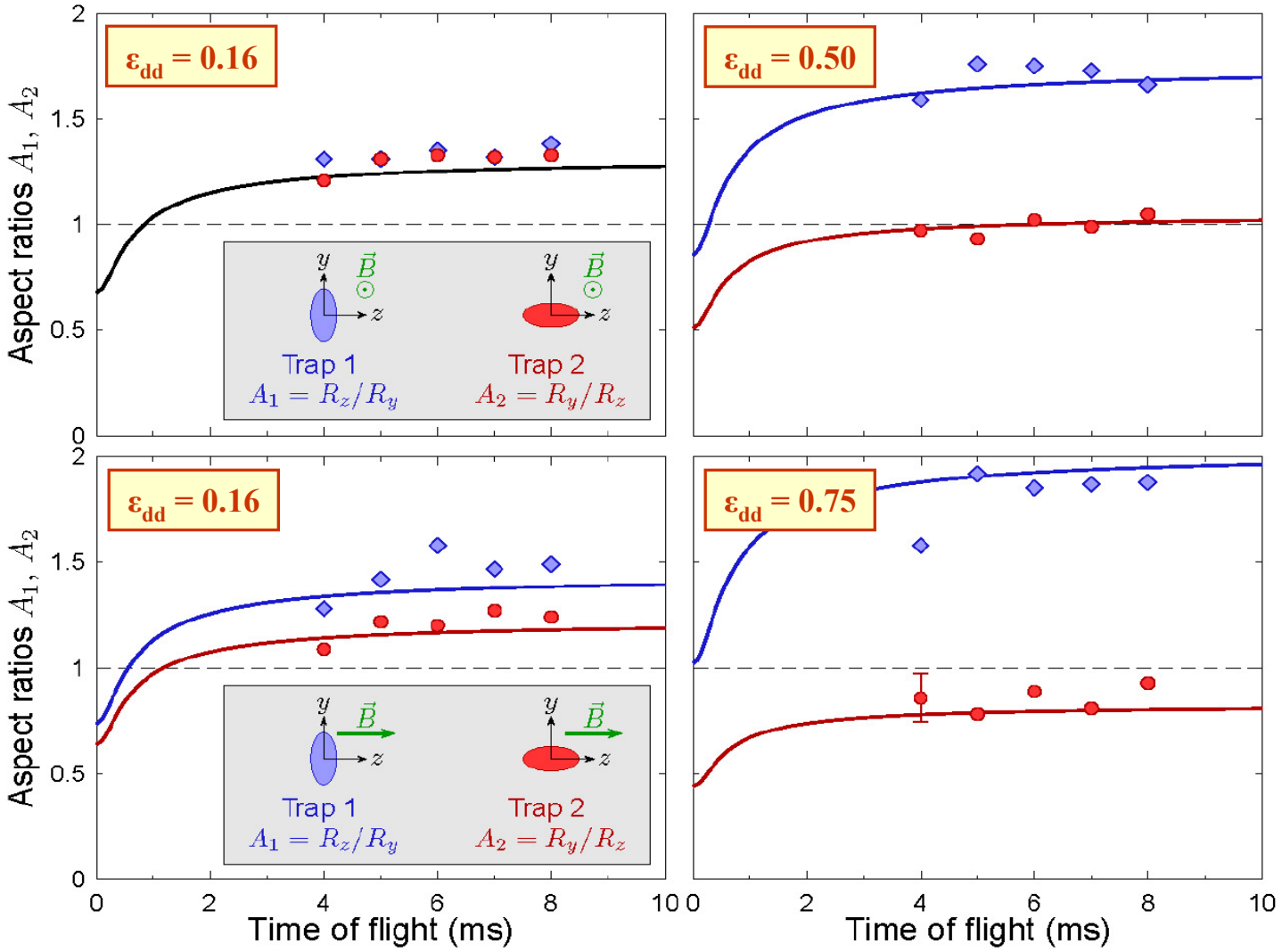

Inhibition of the inversion of ellipticity!

T. Lahaye *et al.*, Nature **448**, 672 (2007).

Outline

1. Which dipolar systems?

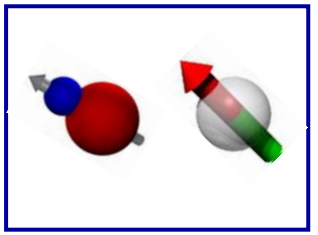

2. Demagnetization cooling

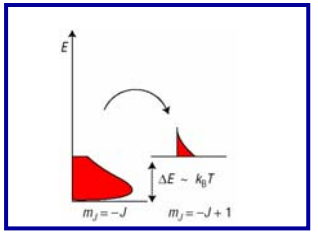

3. Expansion of a quantum ferrofluid

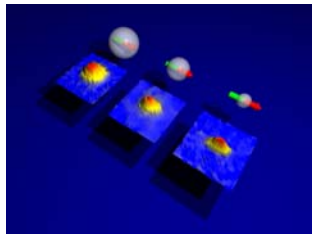

4. **Dipolar collapse**

Preliminary data!

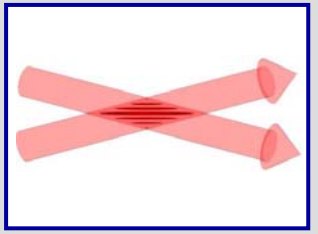

Contact interaction: BEC collapse for $a < 0$

Uniform case: a BEC with $a < 0$ is unstable.

In a trap: a BEC with $a < 0$ cannot accommodate more atoms than the critical value (for an isotropic trap)

$$\frac{N_{\rm crit}|a|}{a_{\rm ho}} = 0.57$$

Simple model: Gaussian Ansatz

$$\phi(r) = \left(\frac{N}{w^3 a_{\rm ho}^3 \pi^{3/2}}\right)^{1/2} \exp\left(-\frac{r^2}{2w^2 a_{\rm ho}^2}\right)$$

$$\frac{E(w)}{N\hbar\omega_{\rm ho}} = \frac{3}{4}(w^{-2}+w^2) - (2\pi)^{-1/2}\frac{N|a|}{a_{\rm ho}}w^{-3}$$

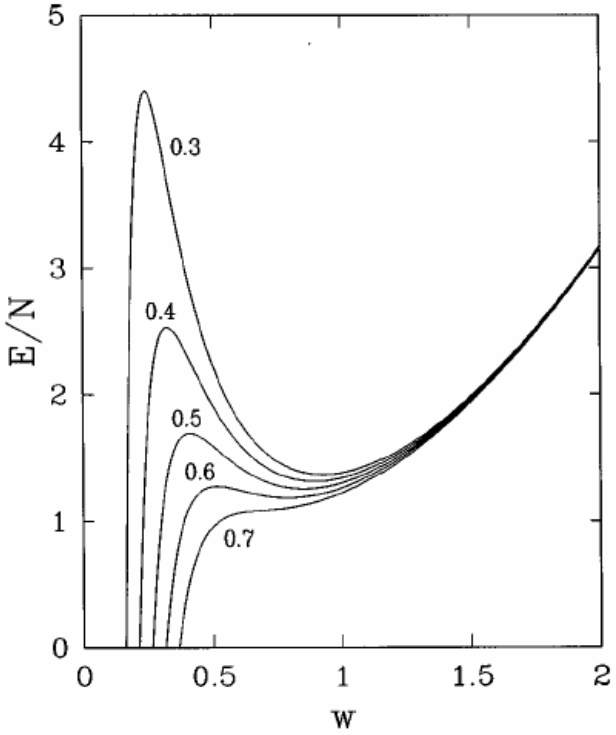

Experiments: ^{7}Li (Hulet's group) and ^{85}Rb (Wieman's group)

Dipolar collapse

The stabiltiy of a dipolar BEC depends on the trap geometry

$$V(x,y,z) = \frac{m}{2}\left[\omega_\rho^2(x^2+y^2) + \omega_z^2 z^2\right]$$

Aspect ratio: $\lambda \equiv \dfrac{\omega_z}{\omega_\rho}$

Cigar-shaped trap:

$\lambda < 1$

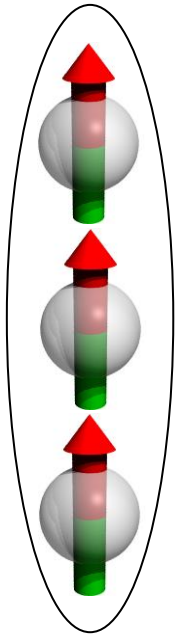

Pancake-shaped trap: $\lambda > 1$

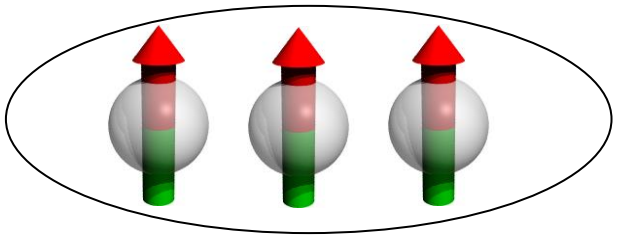

MDDI effectively **attractive**:
unstable

MDDI effectively **repulsive**:
stable

Experimental setup

Superimpose a long-period optical lattice onto the ODT

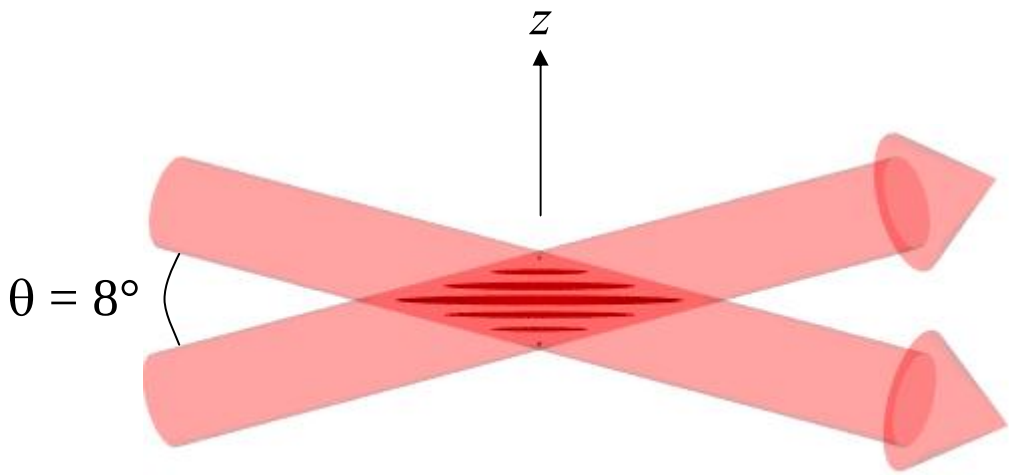

- Monomode fibre laser at 1064 nm (IPG), up to 20 W.
- Lattice period 7 µm. $d = \frac{\lambda_L}{2\sin(\theta/2)}$
- Extra radial confinement by ODT.
- Vary trap aspect ratio λ from 1/10 (no lattice) to 20.
- Load one or two sites.

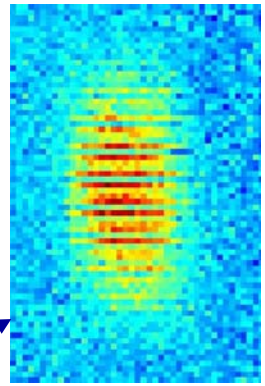

Onset of instability for different traps

Prepare BEC in a trap with given λ and then decrease *a*

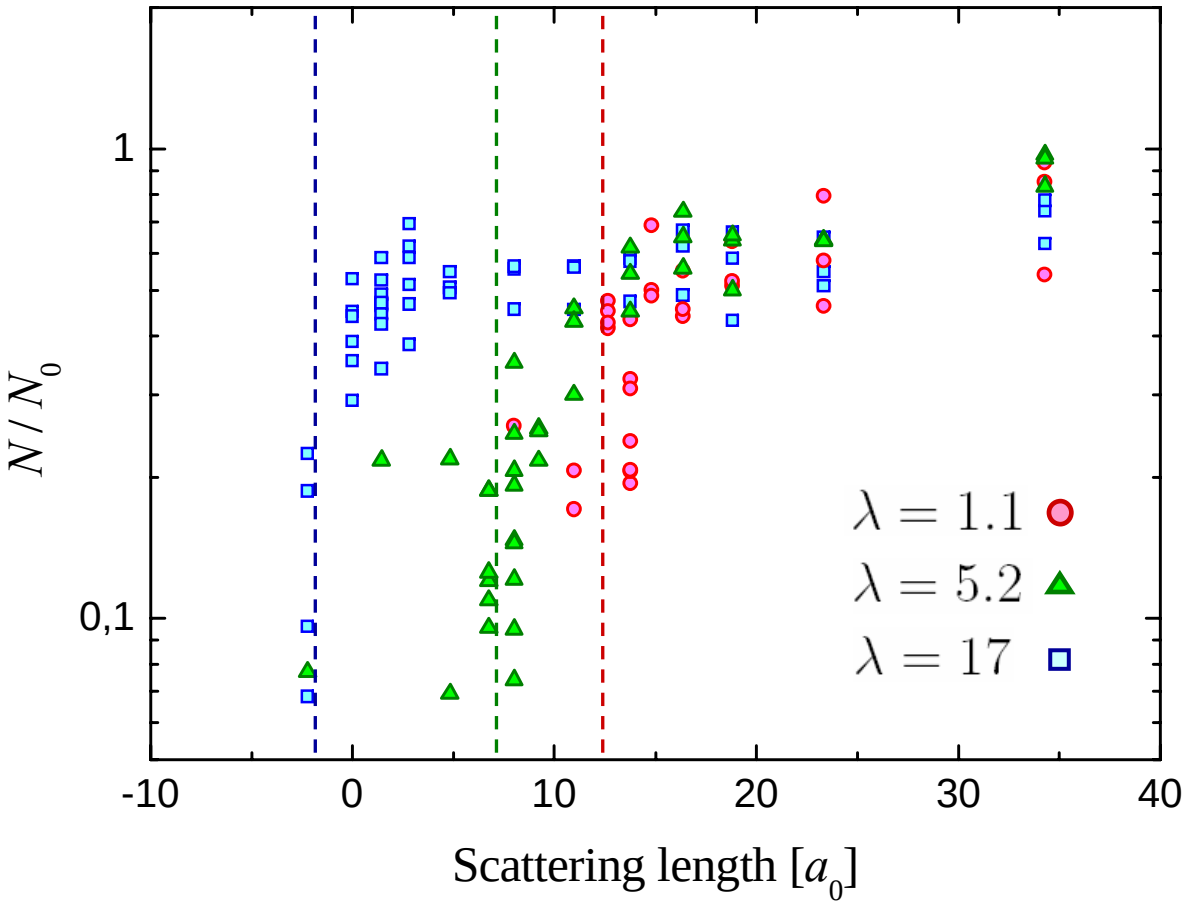

For all traps:

$$\bar{\omega} = (\omega_\rho^2 \omega_z)^{1/3} \simeq 2\pi \times 800\,\mathrm{Hz}$$

Initial N_0 = 20,000

Preliminary data!

Qualitatively as expected: the more pancake, the more stable.

A simple (the simplest) model

How to find easily the critical value a_{crit} for instability?

→ Gaussian Ansatz

- Variational parameters: axial and radial widths. N, a, ω_ρ, ω_z fixed.

$$\psi = \mathcal{A} \exp\left(-\frac{x^2+y^2}{2\xi_\rho^2} - \frac{z^2}{2\xi_z^2}\right)$$

- Calculate the Gross-Pitaevskii energy functional.

$$\mathcal{E}[\psi] = \int \left(\frac{\hbar^2}{2m}|\boldsymbol{\nabla}\psi|^2 + V|\psi|^2 + \frac{g}{2}|\psi|^4 + \frac{1}{2}|\psi|^2 \int U_{\mathrm{dd}}(\boldsymbol{r}-\boldsymbol{r}')|\psi(\boldsymbol{r}')|^2 \,\mathrm{d}\boldsymbol{r}'\right) \mathrm{d}\boldsymbol{r}$$

- Find the value of a for which no local minimum exists: this defines a_{crit}.

Geometry-dependent stability

Preliminary data!

a_{crit} vs trap aspect ratio

(N = 20,000 atoms; $\bar{\omega} \simeq 2\pi \times 800\,\mathrm{Hz}$)

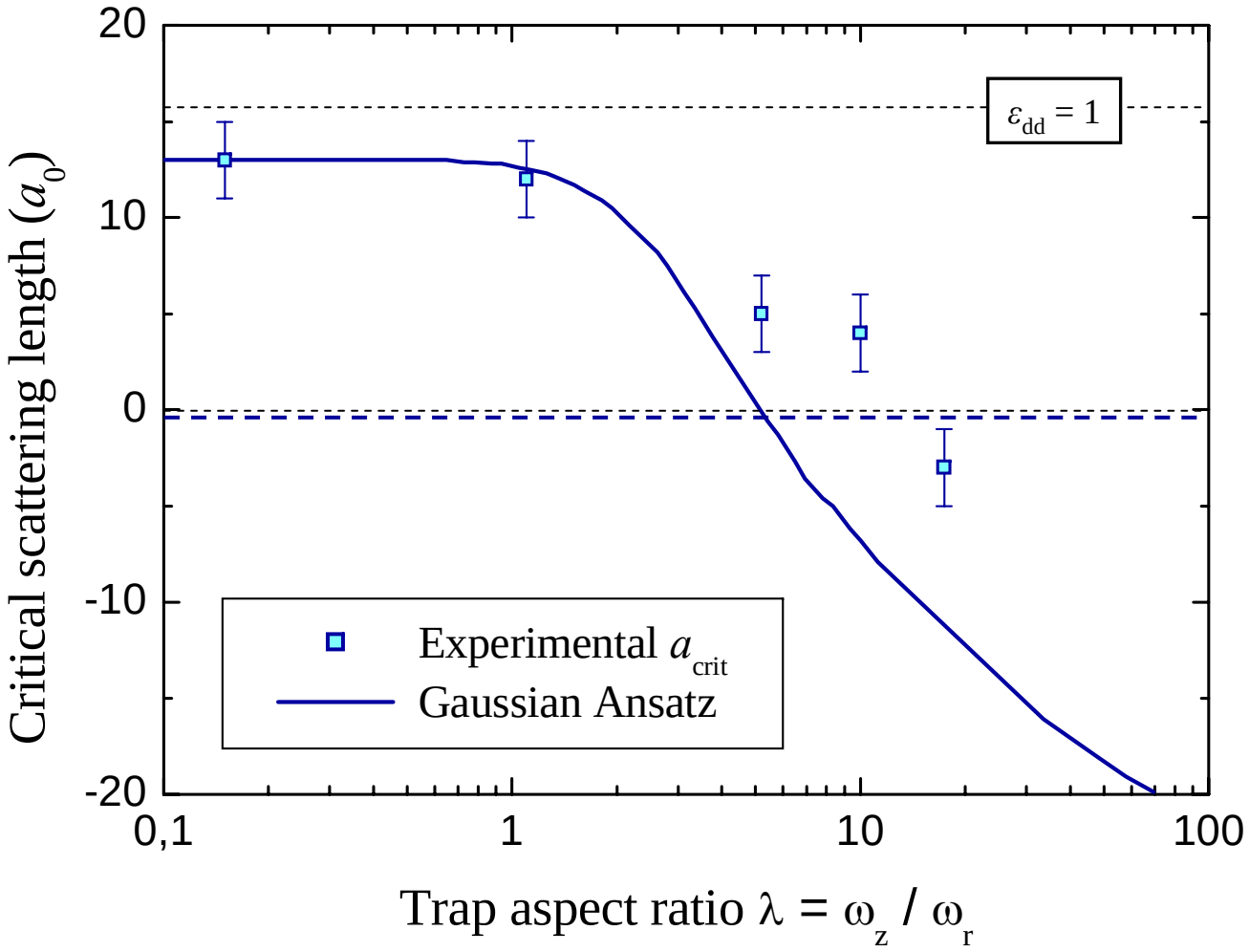

Outlook

- **Dynamics of the collapse**

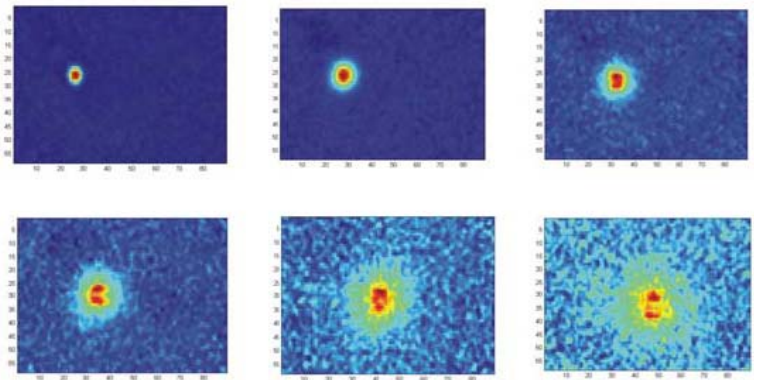

- **Elementary excitations in a pancake trap**
  Roton minimum

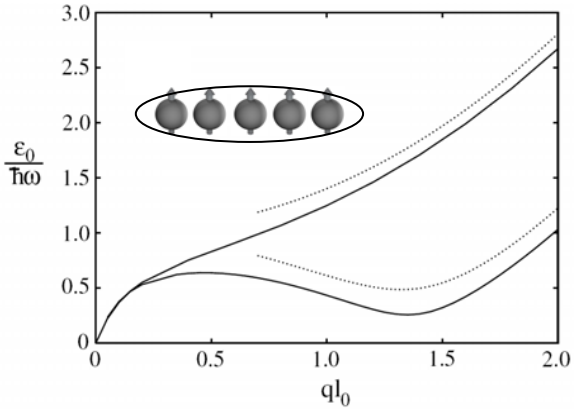

- **Effects of MDDI in a double-well geometry**

- **Three-dimensional optical lattice: towards new quantum phases**

Thanks for your attention!

The Cr team in Stuttgart:

Positions available!

Funding: http://www.pi5.uni-stuttgart.de/

CO.CO.MAT

SFB/TR 21

Deutsche Forschungsgemeinschaft

SPP1116

DFG

MARIE CURIE ACTIONS